REPORT DOCUMENTATION PAGE

Form Approved
OMB NO. 0704-0188

1. AGENCY USE ONLY (Leave Blank)	2. REPORT DATE July 2000	3. REPORT TYPE AND DATES COVERED Final Report

4. TITLE AND SUBTITLE

Polarization-Based Image Understanding Research for Automatic Target Recognition

5. FUNDING NUMBERS

DAAH04-94-G-0278

6. AUTHOR(S)

Lawrence B. Wolff

7. PERFORMING ORGANIZATION NAME(S) AND ADDRESS(ES)

The Johns Hopkins University
Baltimore, Maryland 21218

8. PERFORMING ORGANIZATION REPORT NUMBER

9. SPONSORING / MONITORING AGENCY NAME(S) AND ADDRESS(ES)

U. S. Army Research Office
P.O. Box 12211
Research Triangle Park, NC 27709-2211

10. SPONSORING / MONITORING AGENCY REPORT NUMBER

ARO 33590.1-MA

11. SUPPLEMENTARY NOTES

The views, opinions and/or findings contained in this report are those of the author(s) and should not be construed as an official Department of the Army position, policy or decision, unless so designated by other documentation.

12 a. DISTRIBUTION / AVAILABILITY STATEMENT

Approved for public release; distribution unlimited.

12 b. DISTRIBUTION CODE

13. ABSTRACT (Maximum 200 words)

Major developments in a new promising approach to Automatic Target Detection and Recognition have taken place this year building off of previous research developments in Polarization Vision. Preliminary results have already demonstrated tangible enhanced capabilities for RSTA in the UGV program for Detection of heavily occluded military vehicles, woodland camouflage nets, and, augmented features for Target Recognition. Basic research in Polarization Vision has continued with the development of a material classification method having the capability of detecting metallic materials under polarized illumination of clear skylight, complementary in nature to existing meth-

14. SUBJECT TERMS

15. NUMBER OF PAGES

16. PRICE CODE

17. SECURITY CLASSIFICATION OR REPORT	18. SECURITY CLASSIFICATION ON THIS PAGE	19. SECURITY CLASSIFICATION OF ABSTRACT	20. LIMITATION OF ABSTRACT
UNCLASSIFIED	UNCLASSIFIED	UNCLASSIFIED	UL

NSN 7540-01-280-5500

Standard Form 298 (Rev.2-89)
Prescribed by ANSI Std. 239-18
298-102

ods. New photometric invariants have been discovered for object recognition under multiple light illumination based upon the relationship between the local covariance matrix of photometric values and Gaussian curvature. For 3-D images in Medical Imaging of complex tubular anatomy (e.g., lung bronchial and vascular trees) accurate automated methods have been developed for extraction of central axis geometry which is of large importance to medical researchers.

Polarization-Based Image Understanding Research For Automatic Target Recognition DARPA/ARO contract Final Report

Lawrence B. Wolff
Computer Vision Laboratory
Department of Computer Science
The Johns Hopkins University
Baltimore, Maryland 21218

Abstract

Major developments in a new promising approach to Automatic Target Detection and Recognition have taken place this year building off of previous research developments in Polarization Vision. Preliminary results have already demonstrated tangible enhanced capabilities for RSTA in the UGV program for Detection of heavily occluded military vehicles, woodland camouflage nets, and, augmented features for Target Recognition. Basic research in Polarization Vision has continued with the development of a material classification method having the capability of detecting metallic materials under polarized illumination of clear skylight, complementary in nature to existing methods. New photometric invariants have been discovered for object recognition under multiple light illumination based upon the relationship between the local covariance matrix of photometric values and Gaussian curvature. For 3-D images in Medical Imaging of complex tubular anatomy (e.g., lung bronchial and vascular trees) accurate automated methods have been developed for extraction of central axis geometry which is of large importance to medical researchers.

1 Automatic Target Detection And Recognition

1.1 A New Approach

Polarization vision is an important visual extension to both intensity and color to which human vision is oblivious [13], [15]. There are polarization parameters of light that are physically orthogonal to color and intensity and that are therefore immune to modified or degraded extrinsic "appearance" of objects created by intensity and/or color camouflage, and, clutter. These polarization parameters are instead directly related to the intrinsic material composition, surface roughness, and, shape of objects. This gives strong physical motivation for applying such a sensory modality towards the goal of detecting and recognizing target objects that independent of extrinsic intensity and color appearance have material composition, surface properties and/or geometric properties that differ from surrounding terrain. Decoys (e.g., a painted military vehicle on canvas) that are

made to have the extrinsic appearance of a target may be distinguished in the polarization domain if they differ in material and geometric characteristics from actual targets. As Polarization Vision is an augmentation of intensity and orthogonal to color, sensed polarization of light reflected from military target vehicles naturally provides an augmentation of distinctive signatures that can be used to more accurately recognize a vehicle. Model-based recognition of target vehicles can additionally include polarization signatures taken from a compiled database of empirical polarization imagery for different viewing aspects of the vehicle with respect to different solar-viewing geometries and weather conditions. Such a database is currently being compiled for several military vehicles. Furthermore, polarization reflectance models have been developed incorporating skylight distributed illumination and polarization incident on vehicle surface geometry with specified intrinsic material composition and roughness, accurately predicting salient polarization signatures for vehicles observed in empirical polarization imagery. Not only does this provide a solid physical foundation upon which to base target detection/recognition using polarization signatures, but predictive modeling can enhance recognition and/or detection of vehicles with only knowledge of the physical characteristics of vehicles if empirical image data is absent or incomplete. In the reverse direction, predictive modeling provides constraints on geometry (e.g., pose of a target) and intrinsic material composition that can be derived from observed reflected polarization.

While Polarization Vision by itself for detecting and recognizing targets is not foolproof, preliminary empirical results show that to evade some of the additional capabilities afforded by polarization sensing would require significantly more sophisticated countermeasures than are currently being used. In combination with Automatic Target Detection and Recognition methodologies using other sensor modalities such as multispectral visible and FLIR, as well as LADAR sensing, preliminary experimentation with Polarization Vision appears to provide a new domain of complementary information supporting fusion with these other modalities for increased effectiveness.

1.2 New Sensors For RSTA: Visible, Color, and FLIR Polarization Cameras

Publications in the ARPA IUW Proceedings over the past few years have described progress in the development of new types of fully automated sensors called *polarization cameras* by the Johns Hopkins Computer Vision Laboratory [12], [13]. Recent innovations in modular design have made it possible to build portable Liquid Crystal Polarization Cameras that can rapidly and accurately acquire high resolution polarization imagery outdoors and underwater. Electro-optical switching of liquid crystals in front of a fixed linear polarizer obviates the need for mechanically rotating the polarizer for obtaining polarization component images. Recently we have been able to achieve 10Hz partial linear polarization images doubling our last reported rate of 5Hz.

In the past year Johns Hopkins together with Lockheed-Martin has installed a liquid crystal polarization camera sensor atop a HMMWV (High Mobility Multi-Wheeled Vehicle) scout vehicle at the Lockheed Martin, Denver Colorado facility. See Figure 1. Modular electronic and electro-optical components have been installed directly onto an existing COHU color video sensor used as part of the RSTA sensor suite for the Army/ARPA UGV (Unmanned Ground Vehicle) program. Supporting image acquisition and image processing software were ported to Lockheed-Martin, compatible with the Datacube and VXWorks configuration aboard the three HMMWVs used in the UGV program. Currently, polarization imaging capability is available in the visible spectrum, and for separate Red, Green, and, Blue spectral bands. A number of polarization images have been acquired and some

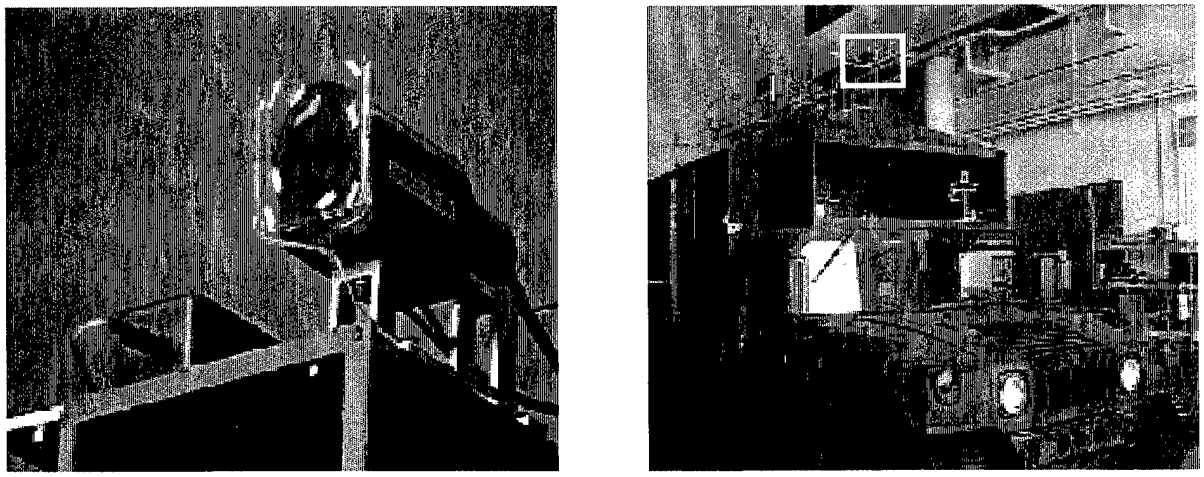

Figure 1: Polarization camera (left) installed on top of a HMMWV scout vehicle (right) at Lockheed-Martin, Denver Colorado Facility. White box in right image shows where camera is located on vehicle.

preliminary results are shown in the next subsection.

Polarization capability is also being added to an existing 3-5 micron FLIR sensor on one of the HMMWV's (also a part of the RSTA sensor suite) at the Lockheed-Martin Denver Facility. Johns Hopkins is currently installing specially customized IR polarization filters that will enable the acquisition of partial linear polarization images for both night operation and analysis of the polarization of thermal emissions from target vehicles.

1.3 Preliminary Empirical Results For Visible Polarization

A large initial dataset of polarization imagery has been collected with the polarization camera shown in Figure 1, of various military vehicles including an Armored Personell Carrier, M-60 tank, Bradley Fighting Vehicle, and M-35 truck. The most comprehensive polarization imagery and analysis has been done on a HMMWV (i.e., separate from the scout vehicles) for various viewing aspects, solar-illumination geometry and weather, and for various levels of occlusion and camouflage with Army Woodland camouflage nets. A more detailed summary of results are shown in a paper in this proceedings [16].

Figure 2 shows intensity and polarization images of a HMMWV vehicle. The polarization image reveals an augmented description in terms of shape and pose constraints on the geometry of the vehicle, with different color hues (grey tones for black-white version) representing orientation of reflected linear polarization directly related to surface normal constraints. Polarization reflectance modeling has been developed that can predict the same polarization-based signature from a geometric, material composition, and, surface roughness model for various portions of the HMMWV as discussed below and in the paper [16]. Not only is this polarization signature quite distinctive with respect to background terrain and other vehicles (e.g., the distribution of reflected linear polarization orientations around a three-way corner at the rear of the vehicle) but it is extremely easy

to distinguish this from a painted canvas decoy which would give a flat single orientation linear polarization signature.

Figure 3 shows an intensity image (left) and a thresholded polarization image (right) of the same HMMWV as in Figure 2 in this scene heavily occluded by high bushes so that only the roof of the vehicle is in direct view. Making up only a small portion of the total area of the scene and blending in with background terrain can make the presence of such a vehicle difficult to detect. A polarization image thresholding out lower degree of polarization (right image) reveals only the roof of the HMMWV in color thresholding it out from background terrain having significantly less degree of polarization. The hue chromaticity (grey tone for black-white version) in this image not only highlights the presence of significant degree of polarization coming from the roof of the vehicle in the scene, but reveals a constraint on how the roof of the vehicle is oriented.

Figure 4 shows an intensity image (left) and a thresholded polarization image (right) of again the same HMMWV but in this scene completely draped with U.S. Army Woodland camouflage nets, and partly occluded by a bush. Even though the camouflage nets have the same color and texture appearance as other background vegetation, reflected polarization is directly related to the intrinsic material composition invariant to intensity/color appearance. The Magenta color (grey tone for black-white version) in the right image is used as a label showing where the degree of polarization is above 0.3 in the scene picking out the camouflage and visually highlighting detection of the target. Apparently man-made materials have polarization properties that are distinct from natural materials. The thresholded polarization images shown in Figures 3 and 4 illustrate how polarization signatures are immune to clutter caused by extrinsic variations in reflected color and intensity. Polarization vision can therefore detect important information that may not be evident with other sensor modalities. It should be noted that the net camouflage in Figure 4 is made to be stealthed to radar.

1.4 Predictive Reflectance Modeling For Outdoor Scenes

Figure 5 shows the predicted orientation of reflected linear polarization under approximately the same skylight illumination distribution as the scene in Figure 2, for two different rendered poses of the HMMWV. The colors (grey tones for black-white version) representing orientation of reflected linear polarization in the left rendered image consistently match those observed in Figure 5. The different colors (grey tones for black-white version) rendered for the left image of Figure 5 demonstrates how the orientation of reflected linear polarization is strongly dependent upon the pose of the HMMWV. In fact, for views of a vehicle where multiple surface orientations are visible (typically 2 or more surface orientations) the pose of the vehicle may be accurately estimated through consistent matching of reflected polarization orientations. For instance, while the orientation of reflected polarization is the same for the roof of the vehicle in both poses, other visible surface orientations produce significantly different orientations of reflected linear polarization. This can be combined with more classical approaches to pose estimation using geometric projection. Comparing the pose of the HMMWV rendered in the right image with the polarization image of Figure 2 illustrates a good pose estimation. There are no other poses producing a nearly consistent combination of orientations of reflected linear polarization.

Take note that while the windows and side panel on the right side of the HMMWV vehicle have similar surface orientation, the orientation of reflected linear polarization is significantly different

Figure 2: Intensity Image (left) and Polarization Image (right) of a HMMWV under partly cloudy sky with sun obstruction.

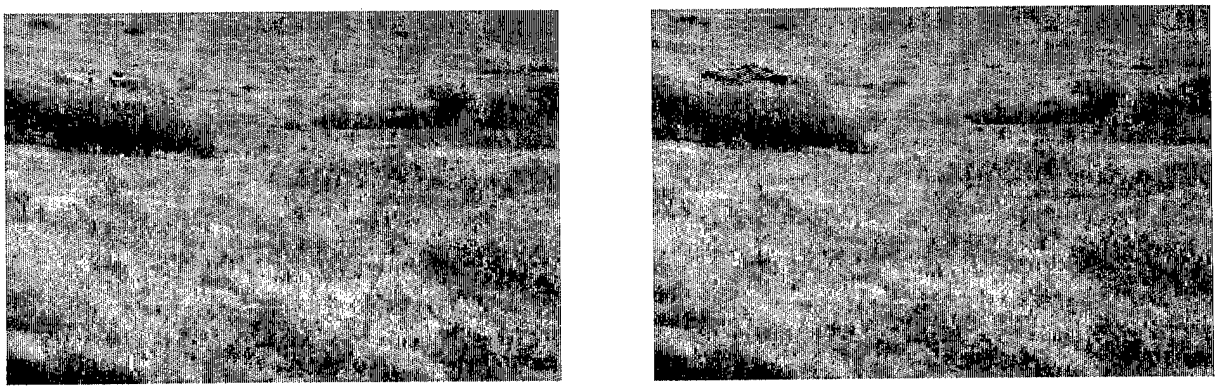

Figure 3: Intensity Image (left) and thresholded Polarization Image (right) of a HMMWV heavily occluded by vegetation under a sunny sky.

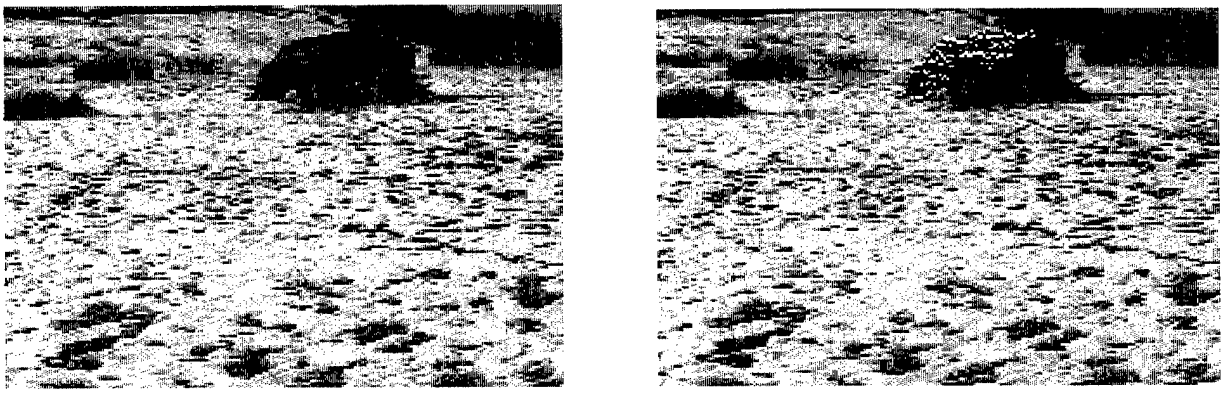

Figure 4: Intensity Image (left) and thresholded Polarization Image (right) of a HMMWV partly occluded by vegetation and with U.S. Army Woodland Camouflage draped over the top, under sunny sky.

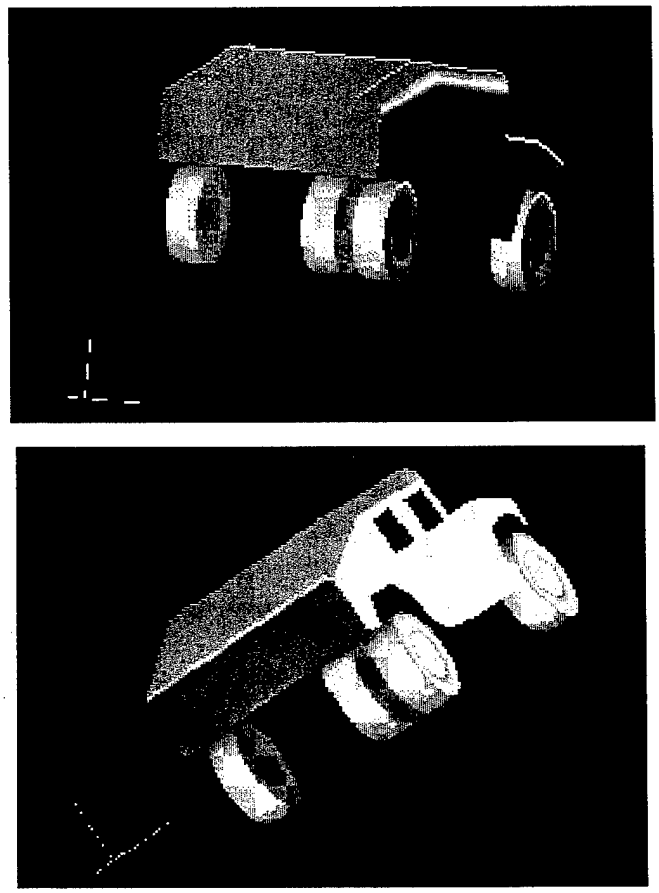

Figure 5: Rendered polarization images for two poses of HMMWV under same sky illumination conditions as in Figure 2 from predictive polarization reflectance modeling (back and hind of wheels are in shadow)

due to the window surface being smooth and the painted side panel being rough and therefore "averaging" the reflected polarization of light incident from multiple directions. This demonstrates the significant dependence of the orientation of reflected linear polarization upon surface characteristics such as roughness. Predictive reflectance modeling of this sort is important for physically understanding polarization signatures towards the goal of recognition and detection. More details in [16].

2 Basic Research In Polarization Vision

While Johns Hopkins is building upon previous basic research in polarization vision for application to Automatic Target Detection and Recognition, basic research into novel methodologies for polarization vision continues.

2.1 Polarization-based Material Classification Under Polarized Illumination

In [10], [11], a practical polarization-based technique was developed that could differentiate at a pixel in an image materials according to electrical conductivity, with metal (electrically conducting) and dielectric (non-electrically conducting) at the extremes. This technique is based upon the relationship between the measurement of the ratio of maximum and minimum polarization components and the *polarization Fresnel ratio*, under the assumption of unpolarized incident illumination. A disadvantage of this polarization-based method is that it becomes inaccurate when the diffuse component of reflection is not small compared with the specular component. For instance, this method will misclassify highly diffuse white paper as metal. Because this previous polarization-based method assumes incident unpolarized light, detection of metallic objects illuminated by the partially linear polarized light from clear or partly cloudy sky (e.g., for automatic target detection and recognition) has also been a problem.

A recently developed technique by Chen and Wolff [3] based upon the polarization *phase* of a light wave, has been shown to function quite well under almost all conditions which have been previously problematic to the above existing material classification technique. The phenomenon of polarization phase is seen in varying states of elliptical polarization where the shape and orientation of the ellipse is determined by the relative phase difference between orthogonal light wave components (e.g., circular polarization results from orthogonal light waves being 1/4 wavelength relatively phase shifted). Polarization phase has been used before to aid in the determination of surface orientation for dielectric objects [7]. The distinction between metal and dielectric with respect to phase of polarization is that metal retards light waves and therefore alters the phase of polarization of incident light upon specular reflection whereas dielectrics do not at all alter the phase of polarization of incident light. For instance, linearly polarized incident light will become elliptically polarized when reflected from a metal, but remain linearly polarized when reflected from a dielectric. The distinction between metal and dielectric material is therefore determined by whether there is a measurable retardance between the polarization phase of incident and reflected light with respect to an object. One way of measuring phase retardance is by measuring all four Stokes parameters of polarization such as what is accomplished in precise measurements for astronomy observations or by a measurement apparatus used in [7]. Such an experimental approach is usually unacceptable in a number of machine vision applications where either real-time response is required or the scene can move or change rapidly. An experimental advance is presented in [3] whereby a much simpler methodology for measuring retardance without having to measure all four Stokes parameters that

is extremely sensitive to small shifts in phase. Furthermore, this experimental methodology can be performed utilizing a trivial modification to existing polarization sensing cameras [18] by affixing a quarterwave plate, making it possible to implement this technique at near real-time rates.

The new polarization phase based technique by Chen and Wolff [3] is applicable to scenes where incident illumination contains any non-zero magnitude component of linear polarization at any orientation except parallel or perpendicular to the plane of incidence. These illumination conditions are complementary to the existing polarization-based technique [11] where incident illumination is unpolarized. A key advantage of this polarization phase-based technique is that it can be utilized to determine metal/dielectric objects illuminated outdoors by a clear or partly cloudy sky, as skylight is partially linear polarized according to Rayleigh's Law [2]. Combined with the existing polarization-based method which can detect metal/dielectric objects under cloudy (unpolarized) skies these methods can provide important information for automatic target detection and recognition algorithms under almost any sky condition. Another key advantage of the presented polarization-based technique is that even if specular reflection from a conductive surface is accompanied by a much larger diffuse reflection component, the measurement of retardance is limited only by the signal-to-noise ratio of the camera sensor being larger than the ratio of diffuse to specular reflection. This technique is so sensitive to the retardance of the linear polarized component, that phase shifting can be detected for most metals close to normal incidence, and close to grazing. In the laboratory where lighting is easily controlled, material classification performs very accurately using this technique.

2.2 Technology Transfer of Polarization Vision For Better Accuracy Of Laser Scanner Range Finders

A popular method for deriving depth maps of shiny objects, such as metallic machine parts, is by triangulation using a laser scanner. The derivation of depth depends upon the assumed geometry of mirror specular reflection. Unfortunately a fundamental problem of obtaining accurate depth maps of highly specular objects in this manner is that there are commonly second and higher order specular inter-reflections. If inter-reflections are falsely interpreted as primary mirror specular reflection, then computed depth will be highly inaccurate since the inter-reflection arises from falsely assumed geometry.

Researchers at Heriot-Watt University, Edinburgh, Scotland are currently developing a laser scanning range finder system incorporating polarization vision techniques for distinguishing primary specular reflections from higher order reflections [4], [5]. Johns Hopkins Computer Vision Laboratory has been collaborating on the theoretical aspects of this work. The basic concept is that the polarization state of higher order specular reflections is quite distinct from that of primarily specularly reflected light.

3 Surface Covariance and Gaussian Curvature: An Invariant Local Descriptor For Object Recognition

Past work by Wolff and Fan [17], and, Fan and Wolff [6] developed multiple illumination methods for identifying hyperbolic, parabolic, and, elliptical points (i.e., points of negative, zero, and positive Gaussian curvature respectively) with only very approximate knowledge of incident illumination. Such local characteristics at points on smooth objects are important due to their invariance to rotation and translation (i.e., pose) of the object, and can be therefore used for object recognition.

Recent work by Angelopoulou et al. [1] uses multiple illumination with only approximate knowledge of incident direction of such illumination to produce a richer description of local curvature for the purpose of object recognition. Under the assumption of Lambertian reflectance (shown to be a good approximation under restricted conditions [14]) it is shown that the determinant of the covariance matrix at each pixel formed from the local image neighborhood of photometric triples is an invariant with respect to rotation of a smooth object, and that the determinant of this covariance matrix is proportional to the absolute value of the Gaussian curvature at a surface point. The distribution of the determinant of the covariance matrix is seen to be a stable signature over a wide range of poses for a given object, and such signatures vary significantly for objects of different shape. To make this signature scale invariant with respect to object size, Angelopoulou et al. [1] compute the medians of quantiles over the distribution (e.g., the median of the lowest 10% of determinant values for the covariance matrix, the median of the next 10% of values, etc...). Figures 6 and 7 show empirical results for different poses of a golf tee and a mug, respectively, the larger the determinant of the local covariance matrix, the darker the value. The presence of specularities gives the appearance of increased curvature (darker values). The graph in Figure 8 takes the medians in deciles and shows the stability of these signatures over the range of the poses shown. Note the difference in the graph signatures.

4 Geometric Analysis of Complex Tubular Anatomy in 3-D Medical Imaging

The capability of accurately extracting geometric features from 3-D medical imagery is becoming more and more important for medical diagnosis. Geometric analysis of complex tubular anatomical structures is important for analysis of lung bronchial trees and vascular structures. An important aspect of this is accurate derivation of the geometry for the "central axis tree" for the tubular structure (e.g., from which the angles of bifurcations can be directly computed). We have taken two approaches to the computation of the central axis tree for complex tubular anatomy, the first involves region growing and optimization, Chandrasekhar et al. [8] the second involves a vector field formulation Williams and Wolff [9]. These methods have in common that they either derive or utilize the centroid points of cross section areas along the tubular structure.

4.1 Derivation of Central Axis Using Region Growing and Optimization

Starting from the root of the tubular tree structure an expanding region is grown out (Top-Down) to establish the topological connectivity along the tree. Once connectivity has been established a second pass grows an expanding region from each of the bottoms of the tree structure (Bottom-Up), the local orientation of the expanding boundary front for these growing regions defining a cut plane along the tree. Growing from Bottom-Up if two branches meet at a node (guided by the connectivity information established on the first pass Top-Down), the new center of expansion becomes that bifurcation node. The centroids of the respective cut-planes are computed and a least squares optimization fitting of straight axes meeting in a 3-way junction is computed. This proceeds all the way back up the tree. This is pictorially summarized in Figure 9

4.2 Derivation of Central Axis Using A Vector Field Approach

The main concept here is to extract a vector "flow field" along the tubular structure for which cut planes are determined to be the most normal too. The centroid points of these cut planes define the central axis with the flow field vector at each point defining the orientation along the central

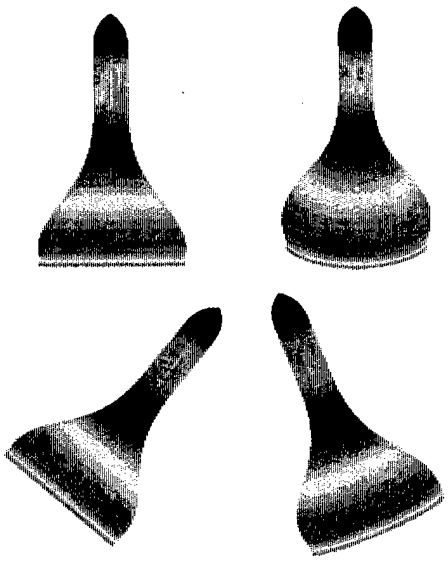

Figure 6: Relative size of the determinant values for the local covariance matrix for different poses of a golf tee (dark-high value, light- low value).

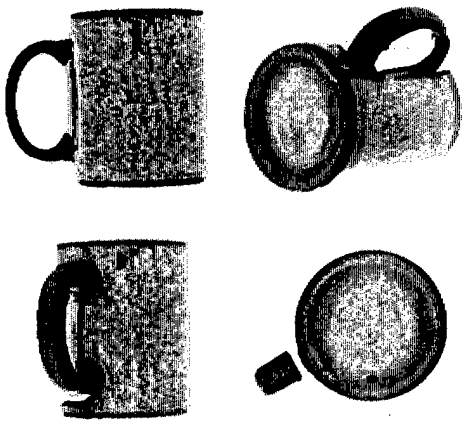

Figure 7: Relative size of the determinant values for the local covariance matrix for different poses of a coffee mug (dark-high value, light- low value).

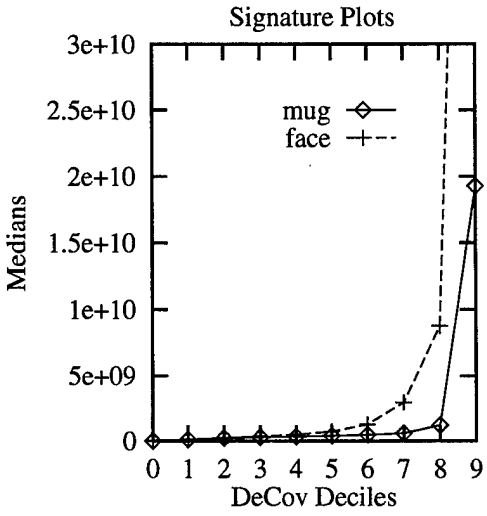

Figure 8: Graph of the deciles of the determinant values for the local covariance matrix (DeCov) for golf tee and coffee mug.

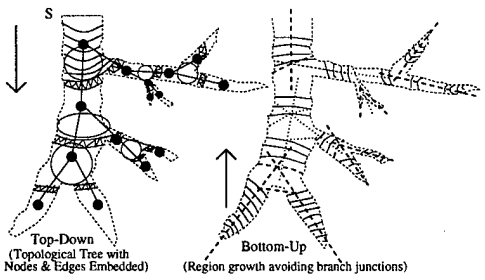

Figure 9: Pictorial summary of region growing and optimization method for central axis tree derivation.

axis. This approach is perhaps more general due to its additional suitability for tubular structures that are curved, such as for vascular trees. The vector flow field is derived from the "escape vector field" which at each point in the tubular tree volume defines the direction of the least distance to escape from the volume. The flow vector at a point in the tubular structure volume is the vector most normal to the escape vectors within a local 3-D neighborhood of that point. Figure 10

References

[1] E. Angelopoulou, J. Williams, and L.B. Wolff. Curvature based signatures for object description and recognition. *Proceedings of the DARPA Image Understanding Workshop*, February 1996.

[2] M. Born and E. Wolf. *Principles of Optics.* Pergamon Press, 1959.

[3] H. Chen and L.B. Wolff. A polarization phase-based method fpr material classification and object recognition in computer vision. *Proceedings of the DARPA Image Understanding Workshop*, February 1996.

[4] J. Clark, E. Trucco, and H.-F. Cheung. Improving laser triangulation sensors using polarization. In *Proceedings of the IEEE Fifth International Conference on Computer Vision (ICCV)*, pages 981–986, Cambridge, Mass., June 1995.

[5] J. Clark, E. Trucco, and L.B. Wolff. Using light polarization in laser scanning. *Invited Submission to Image and Vision Computing Journal*, 1995.

[6] J. Fan and L.B. Wolff. Surface curvature from integrability. In *Proceedings of IEEE Conference on Computer Vision and Pattern Recognition (CVPR)*, pages 520–526, Seattle, Washington, June 1994.

[7] K. Koshikawa and Y. Shirai. A model-based recognition of glossy objects using their polarimetric properties. *Advances in Robotics*, 2(2), 1987.

[8] P. Chandrasekhar L.B. Wolff W. Mitzner and E. Zerhouni. A central axis algorithm for 3d bronchial tree structures. In *Proceedings of the IEEE International Symposium on Computer Vision*, Coral Gables, Florida, November 1995.

[9] J.P. Williams and L.B. Wolff. Form from function: A vector field based approach to the analysis of ct images. In *Proceedings of IEEE Workshop on Physics-Based Modeling in Computer Vision*, pages 70–77, Cambridge, Mass., June 1995.

[10] L.B. Wolff. Material classification and separation of reflection components using polarization/radiometric information. In *Proceedings of the DARPA Image Understanding Workshop*, pages 232–244, May 1989.

[11] L.B. Wolff. Polarization-based material classification from specular reflection. *IEEE Transactions on Pattern Analysis and Machine Intelligence (PAMI)*, 12(11):1059–1071, November 1990.

[12] L.B. Wolff. Polarization camera technology. In *Proceedings of the DARPA Image Understanding Workshop*, pages 1031–1036, Washington, D.C., April 1993.

[13] L.B. Wolff. Advances in polarization vision. *Proceedings of the DARPA Image Understanding Workshop*, November 1994.

[14] L.B. Wolff. A diffuse reflectance model for smooth dielectrics. *Journal of the Optical Society of America, (JOSA) A, Special Issue on Physics Based Machine Vision*, 11(11):2956–2968, November 1994.

[15] L.B. Wolff. Applications of polarization camera technology. *IEEE EXPERT*, 10(5):30–38, October 1995.

[16] L.B. Wolff. A new sensor modality for comprehensive battlefield awareness. *Proceedings of the DARPA Image Understanding Workshop*, February 1996.

[17] L.B. Wolff and J. Fan. Segmentation of surface curvature using a photometric invariant. *Journal of the Optical Society of America, (JOSA) A, Special Issue on Physics Based Machine Vision*, November 1994.

[18] L.B. Wolff and T.A. Mancini. Liquid crystal polarization camera. In *Proceedings of the IEEE Workshop on Applications of Computer Vision*, pages 120–127, Palm Springs, California, December 1992.

Figure 10: Central axis tree derived from empirical tubular tree structure using vector field method.